Available online at www.sciencedirect.com
SCIENCE DIRECT®
Journal of Solid State Chemistry 179 (2006) 909–916
JOURNAL OF SOLID STATE CHEMISTRY
www.elsevier.com/locate/jssc

Kinetic analysis of the thermal stability of lithium silicates (Li_4SiO_4 and Li_2SiO_3)

Daniel Cruz[a,b], Silvia Bulbulian[a], Enrique Lima[c], Heriberto Pfeiffer[d,*]

[a]*Departamento de Química, Instituto Nacional de Investigaciones Nucleares, Apdo. Postal 18-1027, México 11801, D.F., Mexico*
[b]*Facultad de Ciencias, Universidad Autónoma del Estado de México, Instituto Literario No 100 Col. Centro C.P. 50000, Toluca, Edo. de Mexico*
[c]*Departamento de Química, Universidad Autónoma Metropolitana, Iztapalapa, Av. San Rafael Atlixco 186, Col. Vicentina, Apdo. Postal 55-532, 09340, México D.F., Mexico*
[d]*Instituto de Investigaciones en Materiales, Universidad Nacional Autónoma de México, Circuito exterior s/n, CU, Del. Coyoacán, 04510, México D.F., Mexico*

Received 13 July 2005; received in revised form 9 November 2005; accepted 11 December 2005
Available online 20 January 2006

Abstract

The kinetics describing the thermal decomposition of Li_4SiO_4 and Li_2SiO_3 have been analysed. While Li_4SiO_4 decomposed on Li_2SiO_3 by lithium sublimation, Li_2SiO_3 was highly stable at the temperatures studied. Li_4SiO_4 began to decompose between 900 and 1000 °C. However, at 1100 °C or higher temperatures, Li_4SiO_4 melted, and the kinetic data of its decomposition varied. The activation energy of both processes was estimated according to the Arrhenius kinetic theory. The energy values obtained were −408 and −250 kJ mol^{-1} for the solid and liquid phases, respectively. At the same time, the Li_4SiO_4 decomposition process was described mathematically as a function of a diffusion-controlled reaction into a spherical system. The activation energy for this process was estimated to be −331 kJ mol^{-1}. On the other hand, Li_2SiO_3 was not decomposed at high temperatures, but it presented a very high preferential orientation after the heat treatments.

Keywords: Activation energy; Diffusion; Kinetic analysis; Lithium silicate; Li_4SiO_4; Li_2SiO_3; Thermal stability

1. Introduction

In recent years, there is a general agreement that lithium ceramics are the best option for tritium production and release through the ^6Li (n_t, α) ^3H reaction [1]. These two properties determine the possible application of a tritium breeder material into the fusion reactors. Moreover, the ideal breeder material must be very stable under mechanical, thermal and chemical conditions, because of the extreme conditions present in the nucleus of the fusion reactor [2,3]. Consequently, the study of different thermodynamic properties is very important [4].

Different ceramics have been studied as tritium breeder materials, such as lithium titanate (Li_2TiO_3), lithium zirconates (Li_2ZrO_3 and Li_8ZrO_6) and lithium silicates (Li_4SiO_4 and Li_2SiO_3) among others [5–7]. Several papers have been published about the syntheses, neutron irradiation performance, thermal stability and tritium release of these ceramics [8–16]. All these materials exhibit advantages in safety, lack of electromagnetic effects and tritium release.

Different kinds of thermal structural analyses have been performed. For example, Hollenberg studied the swelling of lithium ceramics (Li_4SiO_4, Li_2ZrO_3, $LiAlO_2$ and Li_2O) during irradiation [17]. He found that cracking of lithium ceramic pellets in fusion blankets was inevitable. Helium and tritium gases diffuse through different crystal lattices, producing cracks on the pellets. Additionally, Lui and coworkers reported bubble formation in Li_2O irradiated under slightly different conditions, due to the presence of helium atoms formed during the nuclear reaction [18].

On the other hand, studies on lithium silicates (Li_4SiO_4 and Li_2SiO_3) have demonstrated that these materials

*Corresponding author. Fax: +52 55 56161371.
E-mail address: pfeiffer@zinalco.iimatercu.unam.mx (H. Pfeiffer).

0022-4596/$ - see front matter © 2005 Elsevier Inc. All rights reserved.
doi:10.1016/j.jssc.2005.12.020

present good tritium solubility, they are compatible with structural materials and they seem to have adequate thermo-physical, chemical and mechanical stability at high temperatures [11,19]. The syntheses of lithium silicates have been carried out using different methods, including sol–gel, precipitation, extrusion–spherodisation process, rotating melting procedures, combustion and solid-state reaction [7,11,13,16,20]. Li_2SiO_3 presents an orthorhombic crystal structure with $a = 9.392$ Å, $b = 5.397$ Å, $c = 4.660$ Å [21], while Li_4SiO_4 shows a monoclinic crystal structure with $a = 5.297$ Å, $b = 6.101$ Å, $c = 5.150$ Å, and $\beta = 90.25°$ [22]. Additionally, the Li_2O–SiO_2 phase diagram indicates that Li_4SiO_4 and Li_2SiO_3 begin to melt at temperatures slightly higher than 1000 °C [23].

Although lithium silicates have been widely studied, the thermal stability of these ceramics has not been totally analysed. Hence, this paper attempts to study further the thermal stability of Li_2SiO_3 and Li_4SiO_4. The changes in the structure and composition of Li_2SiO_3 and Li_4SiO_4, due to thermal treatments, were analysed in order to obtain kinetic and structural information about their thermal decomposition processes.

2. Experimental section

Lithium silicates were prepared utilizing analytical grade reagents. In order to obtain high-purity Li_2SiO_3 and Li_4SiO_4, two different methods were chosen. Li_2SiO_3 was prepared by the modified combustion method as reported in a previous paper [13]. Lithium hydroxide (LiOH, Merck), silicic acid (H_2SiO_3, Mallinckrodt) and urea ($CO(NH_2)_2$, Merck) were mixed in distilled water. Once the reagents dissolved, the solution was heated at 70 °C, until most of the water evaporated. The mixture was transferred into a crucible, which was heat-treated at 750 °C. The combustion process was completed within 5 min. On the other hand, Li_4SiO_4 was prepared by a solid-state reaction, using lithium carbonate (Li_2CO_3, Sigma) and silicic acid (H_2SiO_3, Mallinckrodt). The reagents were mixed and pestled in an agate mortar. Then, the mixture was heat-treated in a furnace at 800 °C for 4 h. Finally, the powder was remixed, pestled, and it was heat-treated again at 900 °C for 2 h. As seen in Fig. 1, Li_4SiO_4 could not be obtained pure, Li_2SiO_3 was detected in minimum quantities.

Once both lithium silicates were prepared, samples of Li_2SiO_3 and Li_4SiO_4 were heat-treated at 900, 950, 1000, 1100, 1200 and 1400 °C for different times (15, 30 min, 1, 2, 4, 8 and 16 h). Samples were thermally treated on a Barnstead thermoline electrical furnace with an air atmosphere. After each thermal treatment, the powders were air-cooled to room temperature.

The composition and morphology of the powders were identified by X-ray diffraction (XRD), scanning electron microscopy (SEM), thermogravimetric analysis (TGA) and solid state nuclear magnetic resonance (NMR). A diffractometer (BRUKER axs, D8 Advance) coupled to a copper anode X-ray tube was used for XRD. The relative percentages of the various compounds in the ceramics were estimated from the total area under the most intense diffraction peak for each phase identified by the corresponding JCPDS files (Joint Committee on Powder Diffraction Standards). The samples for SEM were analysed in a Phillips microscope (Phillips XL30). The samples were covered with gold to prevent the lack of conductivity.

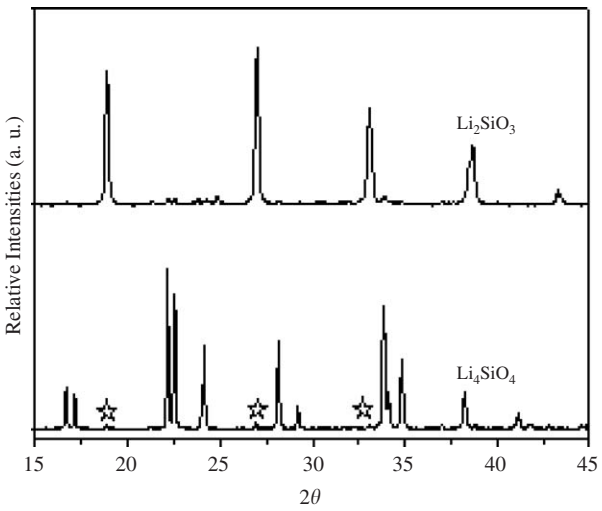

Fig. 1. Powder diffraction patterns of Li_2SiO_3 and Li_4SiO_4 powders after the syntheses processes. Peaks labelled with ☆ correspond to Li_2SiO_3 minor impurities in the Li_4SiO_4 sample.

^7Li and ^{29}Si NMR spectra were obtained in a Bruker ASX 300 spectrometer equipment, with a static field of 7.05 T under magic angle spinning (MAS) conditions, with the spinning rate of 5 kHz. The resonance frequency for ^7Li was $\nu_0 = 116.57$ MHz with a recycling time of 1 s and a single short pulse time of 2 μs. A solution 1 N LiCl was used as the external reference. The ^{29}Si MAS NMR spectra were obtained by operating the spectrometer at 59.59 MHz. The excitation pulse was 3 μs and the delay time, between the pulses, was 8 s. Chemical shifts were referenced to tetramethyl silane (TMS). Finally, a TGA was performed with a heating rate of 10 °C min^{-1} up to 800 °C, flowing N_2 in a TA 51 Thermogravimetric Analyzer.

In order to explain some structural observations, a Li_2SiO_3 theoretical model was built according to the reported structure by Hesse [21]. To elucidate some crystalline planes of the Li_2SiO_3 structure, the model was developed using the crystal building module of CERIUS^2 software [24].

3. Results and discussion

3.1. Synthesis and characterization

Li_2SiO_3, (JCPDS file 29-829) and Li_4SiO_4 (JCPDS file 37-1472), which contain minor impurities of Li_2SiO_3, were obtained by the modified combustion and solid state

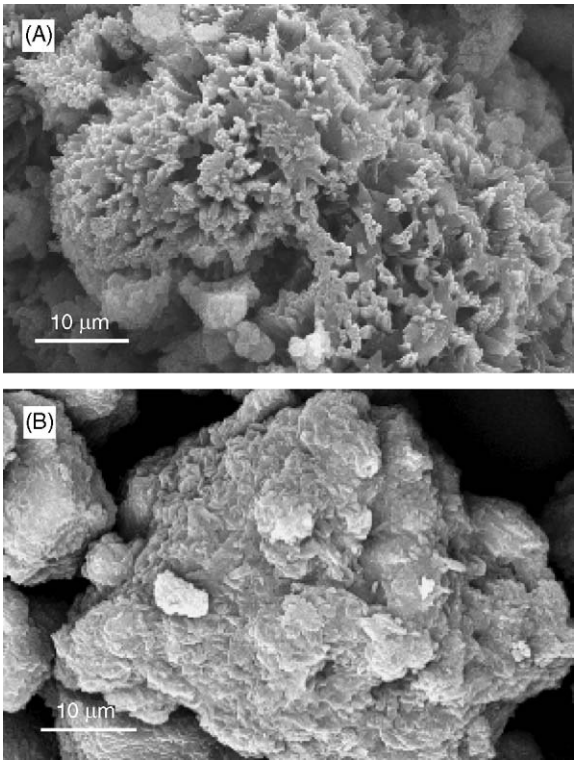

Fig. 2. SEM images of Li_2SiO_3 (A) and Li_4SiO_4 (B) powders.

methods, as shown by XRD (Fig. 1). Fig. 2 shows the SEM images of Li_2SiO_3 and Li_4SiO_4. Li_2SiO_3 powder was formed by agglomerates of 40–50 μm, which were produced by tiny columns growing from the centre of the agglomerates. These particles were very porous (Fig. 2A). On the other hand, Li_4SiO_4 powder showed non-homogeneous polyhedral agglomerates of 50–60 μm (Fig. 2B). These particles seemed to be much denser than the Li_2SiO_3 particles, probably because of a sinterization effect during the long heating process utilized in the solid state method.

TGA curves from room temperature to 800 °C for both ceramics are shown in Fig. 3. Li_2SiO_3 produced by the modified combustion method showed a small reduction of weight between 25 and 200 °C (0.75%) attributed to the dehydration of the sample. A second weight loss, 8.25%, was observed between 450 and 650 °C, which was due to a decarbonation process. Carbon waste could be present in the Li_2SiO_3 surface, as, probably, a 5 min heating period during the synthesis process was not sufficient to eliminate all the carbon compounds produced by the urea combustion.

TGA curve for the Li_4SiO_4 sample, produced by the solid state method, shows that the weight is constant up to 120 °C (Fig. 3). The first reduction of weight was produced between 120 and 280 °C (4.4%), and it was attributed to a dehydration process of water absorbed at the surface of the Li_4SiO_4 particles [11]. A second weight loss was observed between 650 and 750 °C (9.3%) attributed to the decarbonation process, which could be presented as Li_2CO_3 [25]. Actually, it has been reported that Li_4SiO_4 captures CO_2

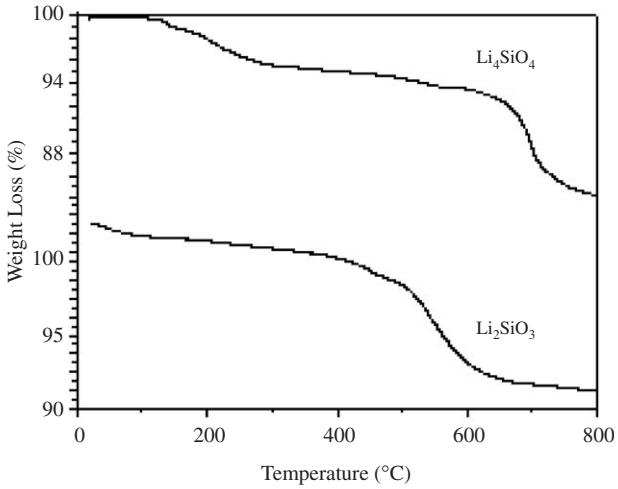

Fig. 3. TGA curves of Li_2SiO_3 and Li_4SiO_4 powders under an atmosphere of N_2.

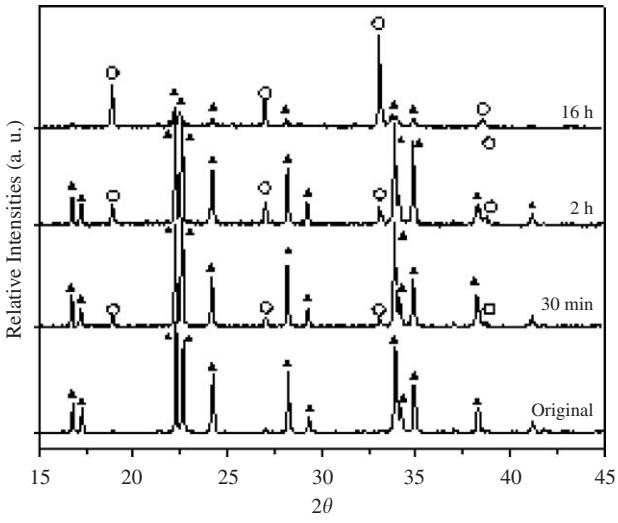

Fig. 4. XRD patterns of Li_4SiO_4 powders heat-treated at 1000 °C for different times. The labels correspond to (▲) Li_4SiO_4 and (○) to Li_2SiO_3, respectively.

even at room temperature, increasing its weight up to 15 wt% just after 20 h [26]. Although the XRD analyses did not show the presence of other compounds than Li_4SiO_4 and Li_2SiO_3, the thermal analyses demonstrated that both materials contained some minor impurities. Note that the lower limit detection by XRD technique depends on the scattering properties of the components of the materials. Silicates, typically, are detected when the concentration is higher than 3%, and the size crystal is bigger than 3 nm.

3.2. *Thermal decomposition of Li_4SiO_4*

Li_4SiO_4 decomposition kinetic data and mechanism were studied at 900, 950, 1000, 1100, 1200 and 1400 °C. As an example, XRD patterns from some of the powders

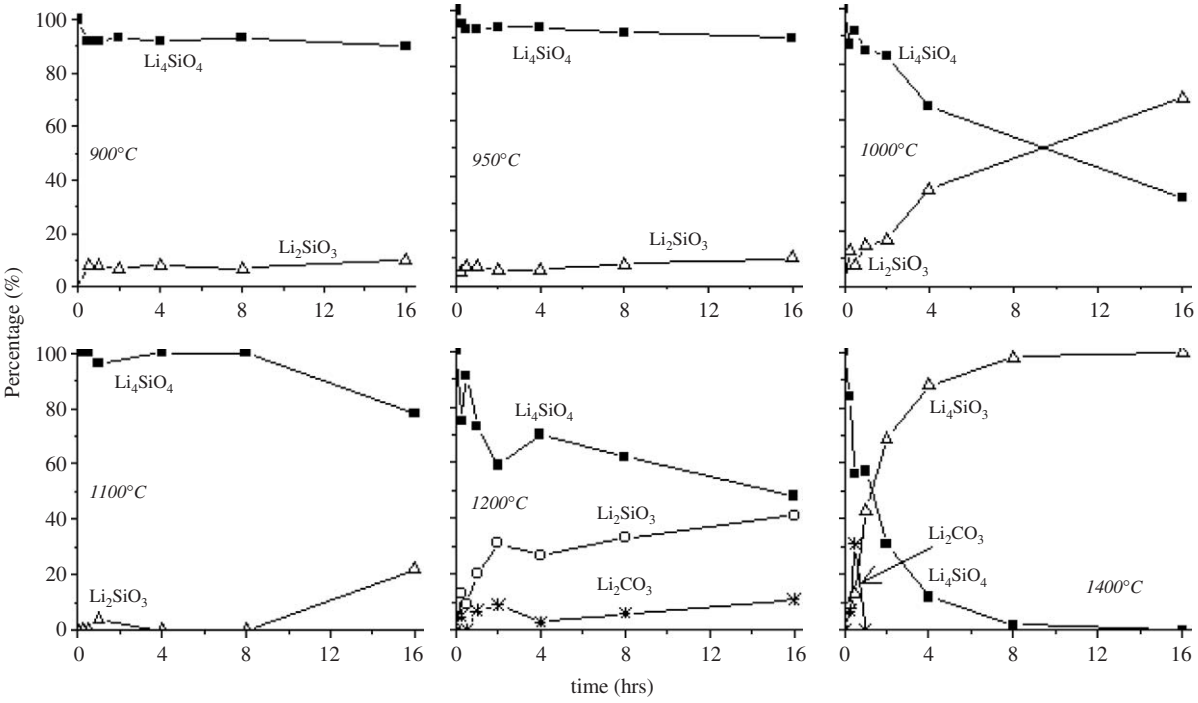

Fig. 5. Percentage of Li_4SiO_4 and the decomposition products (Li_2SiO_3 and Li_2CO_3) as a function of time, at different temperatures.

heat-treated at 1000 °C are shown in Fig. 4. To determine the volume percentage, p, of the compounds detected by XRD, it was assumed that the most intense diffraction peak of each compound was proportional to the percentage in the sample, and it was calculated by Eq. (1):

$$p = \frac{C_i}{\sum_j C} 100, \tag{1}$$

where C_i represents the integral intensity corresponding to each compound identified, and $\sum_j C$ is the addition of the integral intensity corresponding to all the compounds identified in the sample [27]. A summary of the compounds obtained from the Li_4SiO_4 decomposition by XRD, at the different temperatures, is shown in Fig. 5. After 30 min at 900 °C, Li_4SiO_4 began to decompose into small amounts of Li_2SiO_3 (8%). This behaviour was constant up to 8 h of thermal treatment. Several authors have reported that lithium ceramics begin to lose lithium at temperatures higher than 800 °C [9,25,28]. However, at this temperature, there was only a small quantity of lithium that sublimated as Li_2O. Actually, only lithium present at the surface of the Li_4SiO_4 particles must sublimate, and this process takes place according to

$$Li_4SiO_4 \xrightarrow{T} Li_2SiO_3 + Li_2O_{(g)}. \tag{2}$$

Decomposition of Li_4SiO_4 heat-treated at 950 °C, presented a very similar trend to that observed at 900 °C. Nevertheless, the samples heat-treated at 1000 °C showed a faster lithium sublimation. In this case, after only 1 h it was found to change to 15% of Li_2SiO_3. When the sample was heat-treated for 16 h, the composition of the sample changed dramatically to 68% of Li_2SiO_3 and 32% of Li_4SiO_4. Hence, by increasing the temperature, the lithium sublimation kinetic was increased as well, as expected.

However, a totally different behaviour was observed in samples heat-treated at 1100 °C. At this temperature, Li_4SiO_4 changed very slowly, and its decomposition started after 8 h. It means 7 h later than the samples heat-treated at 1000 °C. This behaviour can be explained with the Li_2O–SiO_2 phase diagram [23]. In this diagram, the eutectic temperature of Li_4SiO_4 is 1024 °C. Under the eutectic temperature, Li_4SiO_4 coexists with Li_2SiO_3, but at higher temperatures none of these silicates seems to exist, and, with the exception of Li_4SiO_4, melts. The results in the present work agrees with this information. Samples treated at temperatures lower than 1000 °C were not melted, while samples treated at 1100 °C or higher temperatures melted. As the Li_4SiO_4 melting process absorbs energy, the energy available, for the Li_4SiO_4 decomposition into Li_2SiO_3, should decrease. For this reason, two different kinetic processes were observed, one for the solid state (900–1000 °C) and another for the liquid phase ($T \geqslant 1100$ °C).

When Li_4SiO_4 was heat-treated at 1200 °C, the decomposition rate of Li_4SiO_4 was faster than at 1100 °C. After 4 h, 27% of Li_4SiO_4 was decomposed into Li_2SiO_3. For longer heating periods, 8 and 16 h, Li_4SiO_4 decomposed into Li_2SiO_3 by 32% and 41%, respectively. Moreover, in these samples Li_2CO_3 was also present, at 3% and 11%, respectively. Finally, Li_4SiO_4 samples heat-treated at 1400 °C decomposed rapidly into Li_2SiO_3 and Li_2CO_3. Actually, pure Li_2SiO_3 (100%) was attained after heating the samples for 8 h.

Li_2CO_3 was found in samples heat-treated between 1200 and 1400 °C, but it was not found in samples treated at lower temperatures (900–1100 °C). This behaviour can be explained as follows: it has been reported that Li_4SiO_4 is an excellent CO_2 absorbent at relatively high temperatures (400–600 °C) [26], while Li_2SiO_3 does not seem to absorb CO_2. Thus, the CO_2 absorption must occur during the cooling of the samples, as the samples are air-cooled. The results suggest that the CO_2 absorption by Li_4SiO_4 is favoured in the liquid phase (1200 and 1400 °C), may be because there is more CO_2 trapped during the solidification of the samples.

In order to obtain kinetic information about the decomposition mechanism of Li_4SiO_4, further analyses were performed. Li_4SiO_4 decomposition into Li_2SiO_3 and Li_2O was schematised as a first-order reaction, according to Eq. (2). Then, Eq. (3) was produced, where k is the reaction rate constant. In a first-order reaction, the concentration of Li_4SiO_4 decreases exponentially:

$$-\mathrm{d}[Li_4SiO_4]/\mathrm{d}t = k[Li_4SiO_4], \tag{3}$$

$$\frac{1}{[Li_4SiO_4]}\,\mathrm{d}[Li_4SiO_4] = -k\,\mathrm{d}t, \tag{4}$$

$$[Li_4SiO_4] = A\exp^{-kt}. \tag{5}$$

Fig. 6A represents a plot of $[Li_4SiO_4]$ as a function of time, at different temperatures. The experimental data were fitted to Eq. (5), and then, simulated graphs were extrapolated for longer times. As already described in the previous sections, Li_4SiO_4 decomposition rate increased between 900 and 1000 °C. However, a large reduction of the decomposition rate was observed between 1000 and 1100 °C. For example, while Li_4SiO_4 decomposition process is not completed even after 300 h, at 900 °C, the ceramic treated at 1000 °C decomposes totally only after 50 h. On the other hand, at 1100 °C, Li_4SiO_4 decomposition rate process changes again due to the melting process of the material. At this temperature, lithium orthosilicate again needs almost 300 h for its total decomposition. Finally, at 1200 and 1400 °C, the reaction is accelerated once more, and at 1400 °C, the reaction is completed in only 8 h.

Using the Arrhenius equation, a plot of the ln k vs. $1/T$ should be a straight line. This plot can be seen in Fig. 6B, where two different trends can be clearly observed. The slopes of these two curves correspond to the decomposition activation energies (E_a) of the process, before and after the Li_4SiO_4 melting process. Then, the E_a values for the decomposition of Li_4SiO_4 into Li_2SiO_3, in solid and liquid states, were estimated to be -408 and $-250\,\mathrm{kJ\,mol^{-1}}$, respectively. Therefore, the energy required for Li_4SiO_4 decomposition is higher in solid state. It can be explained by the lithium sublimation, which may be limited by a diffusion process on the solid state.

Actually, if the Li_4SiO_4 decomposition process is limited for the lithium diffusion and later sublimation, this reaction should be described mathematically as a function

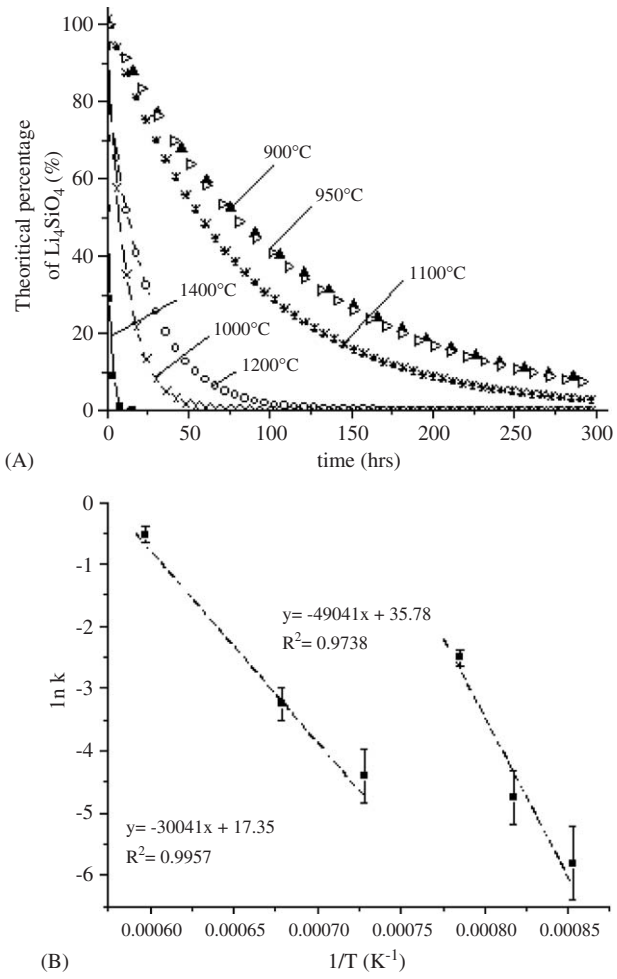

Fig. 6. Kinetic analysis of the Li_4SiO_4 decomposition. (A) Relationship between the Li_4SiO_4 decomposition ratio and time during isothermal heating processes at different temperatures, with the simulated extrapolated curves. (B) ln k vs. $1/T$ for the decomposition of Li_4SiO_4.

of a diffusion-controlled reaction as well. There are several methods that describe a diffusion-controlled reaction depending on geometrical factors. One of these methods is assuming that the diffusion starts on the exterior of a spherical particle of radius r that is reacting from the surface inward [29]:

$$1-(1-r)^{1/3} = k(t-t_0), \tag{6}$$

where r is the thickness of Li_2SiO_3 produced over the Li_4SiO_4 particles at the time t. In this case, only the data obtained between 900 and 1000 °C could be used. This spherical model was chosen because the previous SEM analysis had shown that the Li_4SiO_4 particles have a similar kind of polyhedral geometry. The samples heat-treated at 1100 °C or higher temperatures were melted; therefore, this model cannot be used under these conditions.

Plotting $1-(1-r)^{1/3}$ as a function of time produces the graph of Fig. 7A. The reaction rate constant, k, at the different temperatures was obtained from the slope of each curve. Although the linearity of the plots is not the most adequate, something interesting is that the gradients of the curves improve as a function of the temperature. For a

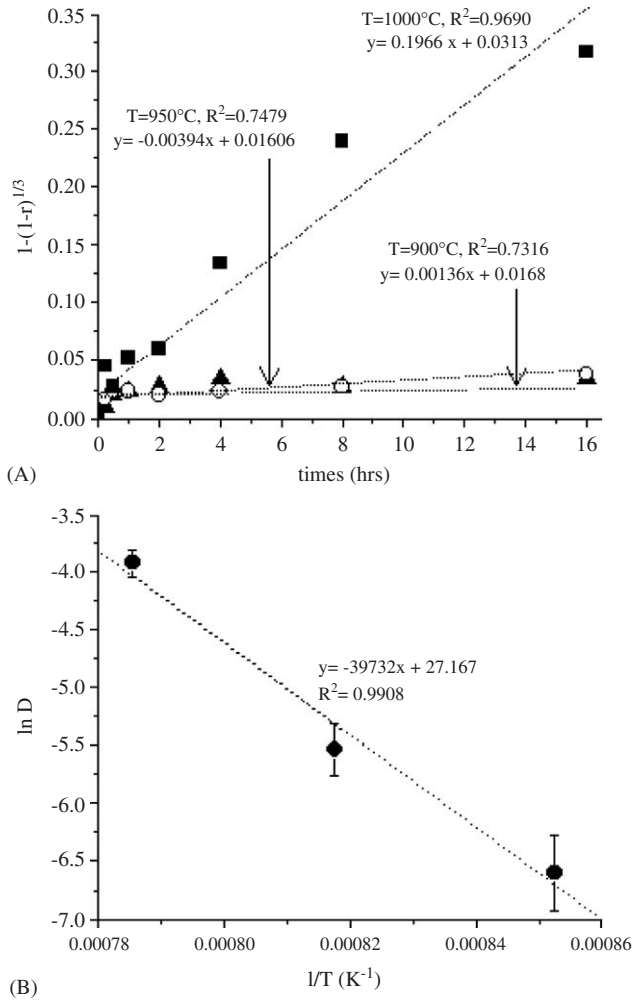

Fig. 7. Diffusion-controlled process for the Li_4SiO_4 decomposition. (A) plot of $1-(1-r)^{1/3}$ against time for the diffusion model and (B) ln D vs. $1/T$ for the decomposition of Li_4SiO_4.

diffusional growth model, the slopes of the lines are proportional to the diffusion coefficient, D, at each temperature. Then, if this mechanism follows an Arrhenius-type behaviour , Eq. (7), a plot of the ln D vs. $1/T$ must be a straight line.

$$D = D_0 e^{-Q/RT}. \quad (7)$$

In this case, the slope of the curve must correspond to the activation energy of the diffusion-controlled reaction process (Fig. 7B). The activation energy value was estimated to be $-331\,kJ\,mol^{-1}$. This activation energy obtained using the spherical diffusion model is $77\,kJ\,mol^{-1}$ smaller than the energy obtained using the kinetic first-order reaction, which corresponds to 18.8% of difference. Some other models were analysed in order to look for a better adjustment between the two theories [29,30]. However, all the different diffusion models analysed gave similar energy values to that obtained with the spherical model. Consequently, the Li_4SiO_4 decomposition could not be limited by a lithium diffusion process.

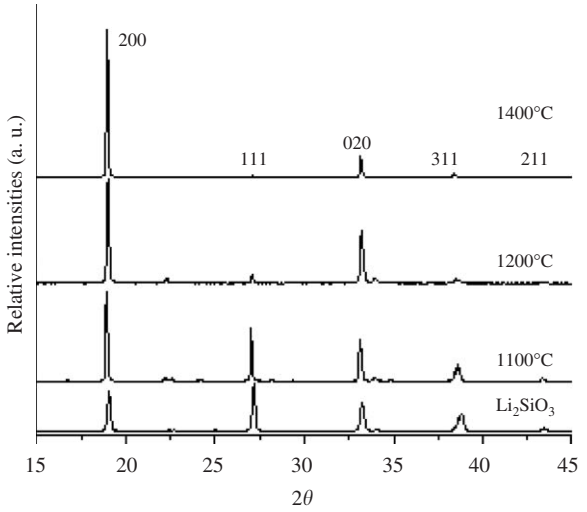

Fig. 8. XRD patterns of Li_2SiO_3 powders heat-treated for 2 h at different temperatures.

3.3. Thermal behaviour of Li_2SiO_3

A set of Li_2SiO_3 samples were heat-treated during various periods, between 1100 and 1400 °C. The samples heat-treated at 1200 and 1400 °C for 60 or more minutes were melted, and they had to be removed from the Pt crucible by scraping it out and pulverising the solid again. Fig. 8 shows the XRD patterns of the powders heat-treated at different temperatures for 2 h. The XRD patterns of Li_2SiO_3 samples, before any thermal treatment, fits with the JCPDS file 29-0829, in which the [111] plane produces the most intense peak at 26.97°. On the other hand, after the heat-treatment at 1100 °C, the intensity of this peak decreases from 100% to 72%. Here, the (200) peak, at 18.87°, becomes the most intense. This second pattern fits another JCPDS file (No. 29-0828), which also corresponds to Li_2SiO_3. Both JCPDS files report the same space group, $Cmc2_1$, and the cell parameters are nearly the same. Hence, the differences between the two structures are only due to a thermal treatment that must produce a preferential orientation effect over the material. In fact, this effect was dramatically favoured at high temperatures (1200 and 1400 °C), as shown in Fig. 8. In both cases, the (111) peak has practically disappeared, and only the (200) and (020) peaks are detectable.

According to the diagram phase of the Li_2O–SiO_2 system, Li_2SiO_3 is partially liquefied at temperatures higher than 1033 °C [23]. Furthermore, as mentioned in the Li_4SiO_4 section, it has been reported that lithium begins to sublimate at $T \geqslant 800$ °C from different lithium ceramics [9,25,29]. Hence, there would be two different hypotheses to explain the decrease of the (111) peak. First, the samples could have been losing lithium by sublimation, preserving its structure, and the second option was that the samples got a very high level of preferential orientation during the melting process.

In order to find out which of the theories was the correct one, different analyses were performed. Initially, Li_2SiO_3

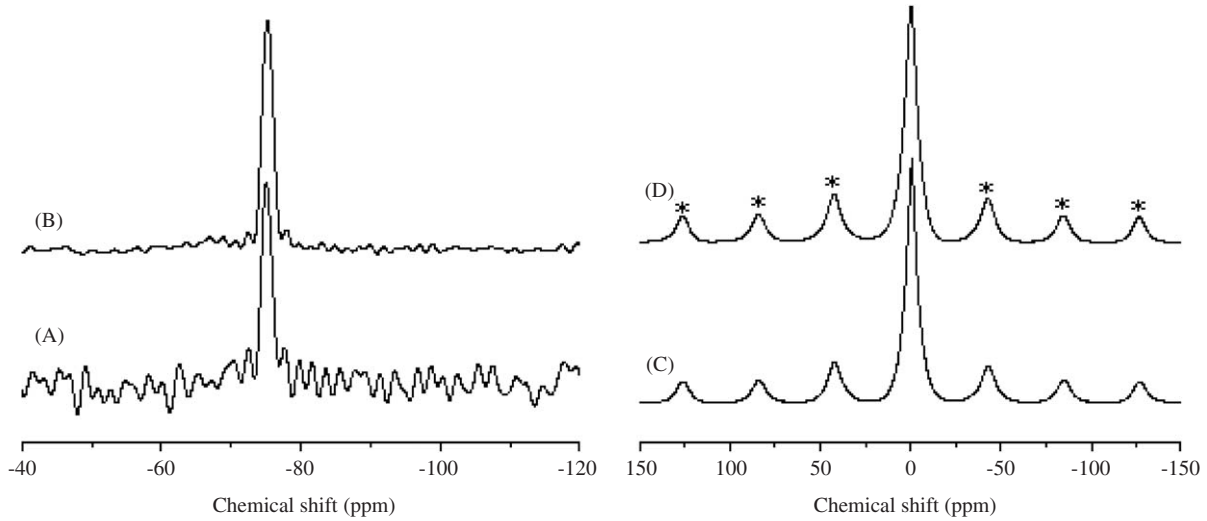

Fig. 9. (A) ^{29}Si MAS NMR spectra of Li_2SiO_3 as synthesized, (B) heat-treated at 1400 °C, (C) ^{7}Li MAS NMR spectra of Li_2SiO_3 as synthesized, and (D) heated at 1400 °C. Peaks labelled (*) indicate spinning bands (rate spinning 5 kHz).

samples, before any thermal treatment, and heat-treated at 1400 °C for 4 h, were analysed by solid-state NMR. Fig. 9A and B display the ^{29}Si MAS NMR spectra for samples unheated and heat-treated at 1400 °C. Remarkably, similar spectra were obtained in both samples. Only one peak at −76 ppm was observed, which is due to Q^2 units [31,32]. Then, the silicates are built only by Q^2 units. In other words, each silicon tetrahedron contains two siloxane bonds (–O–Si) and two non-bridging oxygen atoms, where the negative charge is compensated by the lithium–oxygen ions (–O–Li). Likewise, ^{7}Li MAS NMR spectra show that, as expected, the two samples contain only one lithium site, as only one peak close to 0 ppm is present (Fig. 9C and D). The solid-state NMR analysis strongly suggest that lithium is not being loss.

On the other hand, the sample heat-treated at 1400 °C for 4 h was analysed by SEM (Fig. 10). This study showed the formation of filaments, where its longitude varied from a few microns to hundreds of them. Hence, the solid-state NMR and SEM results confirmed the second hypothesis suggesting that the thermal treatment is promoting the union of several Li_2SiO_3 chains, resulting in the formation of a preferential orientation.

The structure of the $(SiO_3)^{2-}$ silicate is linear, as a chain produced by "n" number of $(SiO_4)^{4-}$ tetrahedrons linked by two oxygen atoms among them [33]. Thus, several of this Li_2SiO_3 chains must be linked, producing the filaments. Fig. 11 shows a $1 \times 2 \times 1$ unit cell model of Li_2SiO_3, in the [001] crystallographic plane. This image clearly shows that the $(SiO_3)^{2-}$ chains are located over the [200] family planes, which are the only planes observed after the thermal treatment on the XRD experimental patterns. Thus, the crystalline structure also confirmed the XRD and solid-state NMR results, where the formation of preferential orientations was suggested. As the filaments are produced by the conjugation of several Li_2SiO_3 chains,

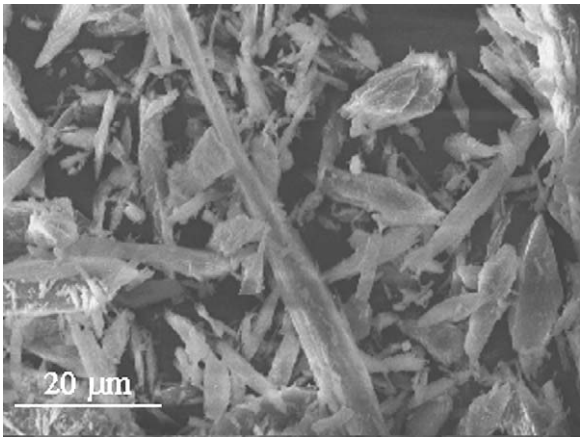

Fig. 10. SEM image of Li_2SiO_3 after a thermal treatment at 1400 °C for 4 h.

these planes become much more populated that any other family planes, inducing the preferential orientation observed by the different techniques.

Hence, both silicates presented different thermal behaviours. While Li_4SiO_4 decomposes on Li_2SiO_3, the structure of Li_2SiO_3 just changed to produce a preferential orientation. Furthermore, these lithium ceramics are more thermally stable than other ceramics such as Li_2ZrO_3, which has been proposed as breeder material for its higher melting point. However, the E_a of the decomposition process is $-210\,kJ\,mol^{-1}$ [9] on solid state, almost $-200\,kJ\,mol^{-1}$ less energy than that required for the Li_4SiO_4 decomposition.

4. Conclusions

The reaction mechanisms and kinetic analyses for the Li_4SiO_4 and Li_2SiO_3 decomposition processes were investigated in this study. Li_4SiO_4 was decomposed into other

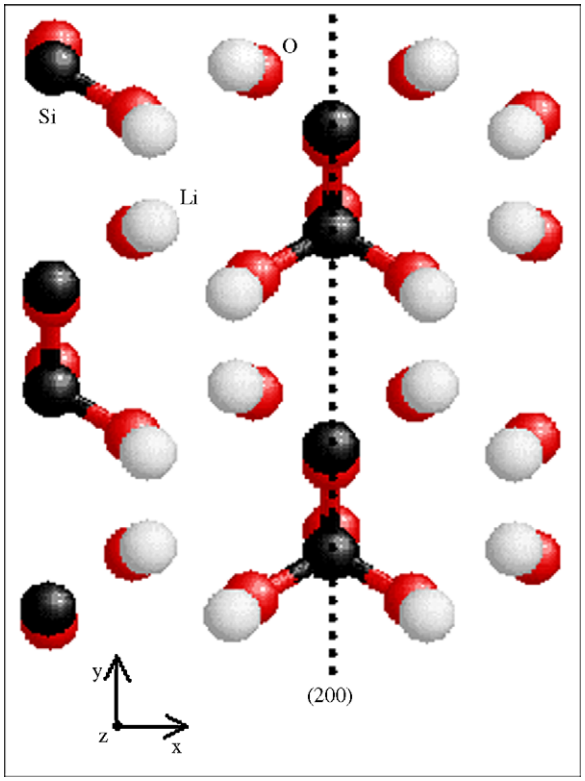

Fig. 11. Scheme of the Li_2SiO_3 structure showing the [200] plane. From the darkest to the highlighted, the spheres represent silicon, oxygen and lithium atoms.

lithium silicates with less quantities of lithium and Li_2SiO_3. Li_4SiO_4 has a tetrahedron structure. Then, some lithium must sublimate as Li_2O while the tetrahedrons link among them to produce chain structures (Li_2SiO_3). The activation energy for this decomposition process was estimated using two different kinds of models. Initially, a first-order reaction model determined that the kinetic decomposition process depends on the physical state of the sample. The activation energies obtained were -408 and $-250\,kJ\,mol^{-1}$ in solid and liquid state, respectively. The difference between the two energies was explained by the lithium diffusion energy required in solid and liquid state. For the solid state samples, a spherical diffusion model was also used. In this case, the activation energy obtained was $-331\,kJ\,mol^{-1}$. Hence, it is possible that Li_4SiO_4 decomposition process is not limited by the lithium diffusion.

On the contrary, Li_2SiO_3 presented a very high level of thermal stability. This material did not decompose, and it was only highly oriented by the union of several $(SiO_3)^{2-}$ chains.

Acknowledgments

D. Cruz thanks the National Council of Science and Technology (CONACYT) of Mexico for financial support. Authors thank L. Baños, L. Carapia and C. Rodriguez for the technical work for the different characterization techniques, XRD, SEM and TGA, respectively.

References

[1] A. Klix, Y. Verzilov, K. Ochiai, T. Nishitani, A. Takahashi, Fus. Eng. Des. 72 (2005) 327–337.
[2] A. Montanaro, J.P. Negro, J. Lecompte, Mater. Sci. 30 (1995) 4335–4338.
[3] M. Nagai, M. Hibino, T. Nishino, K. Noda, J. Mater. Sci. Lett. 12 (1993) 107–109.
[4] H. Kleykamp, Thermochim. Acta 287 (1996) 191–201.
[5] C.E. Johnson, K. Noda, N. Roux, J. Nucl. Mater. 263 (1998) 140–148.
[6] C.E. Johnson, J. Nucl. Mater. 270 (1999) 212–220.
[7] M. Taddia, P. Modesti, A. Albertazzi, J. Nucl. Mater. 336 (2005) 173–176.
[8] C. Alvani, S. Casadio, V. Contini, A. Di Bartolomeo, J.D. Lulewicz, N. Roux, J. Nucl. Mater. 307 (2002) 837–841.
[9] H. Pfeiffer, K.M. Knowles, J. Eur. Ceram. Soc. 24 (2004) 2433–2443.
[10] N. Roux, C. Johnson, K. Noda, J. Nucl. Mater. 191–194 (1992) 15–22.
[11] H. Pfeiffer, P. Bosch, S. Bulbulian, J. Nucl. Mater. 257 (1998) 309–317.
[12] F. Li, K. Hu, J. Li, D. Zhang, G. Chen, J. Nucl. Mater. 300 (2002) 82–88.
[13] D. Cruz, S. Bulbulian, J. Nucl. Mater. 312 (2003) 262–265.
[14] J.J. Kingsley, L.R. Pederson, Mater. Lett. 18 (1993) 89–96.
[15] L.A. Chick, L.R. Pederson, G.D. Maupin, J.L. Bates, L.E. Thomas, G.J. Exarhos, Mater. Lett. 10 (1990) 6–12.
[16] J.G. van der Laan, H. Kawamura, N. Roux, D. Yamaki, J. Nucl. Mater. 283 (2000) 99–109.
[17] G.W. Hollenberg, Adv. Ceram. 25 (1989) 183–193.
[18] Y.Y. Lui, R.F. Mattas, D.L. Smith, D.L. Porter, J. Nucl. Mater. 133–134 (1985) 209–215.
[19] A.R. Raffray, M.C. Billone, G. Federici, S. Tanaka, Fus. Eng. Des. 28 (1995) 240–251.
[20] D. Cruz, S. Bulbulian, J. Am. Ceram. Soc. 88 (2005) 1720–1724.
[21] K. Hesse, Acta Cryst. B 33 (1977) 901–902.
[22] H.F. McMurdie, Powder Diffr. 1 (1986) 334–339.
[23] F.C. Kracek, J. Phys. Chem. 34 (1930) 2645.
[24] Cerius^2, Quantum Mechanics—Physics of Molecular Simulation, San Diego, CA, 1997.
[25] C.H. Lu, L. Wei-Cheng, J. Mater. Chem. 10 (2000) 1403–1407.
[26] K. Essaki, K. Nakagawa, M. Kato, H. Uemoto, J. Chem. Eng. Japan 37 (2004) 772–777.
[27] Y.P. Fu, C.C. Chang, C.H. Lin, T.S. Chin, Ceram. Int. 30 (2004) 41–45.
[28] H. Pfeiffer, P. Bosch, Chem. Mater. 17 (2005) 1704–1710.
[29] J.H. Sharp, G.W. Brindley, B.N. Narahari-Achar, J. Am. Ceram. Soc. 49 (1966) 379–382.
[30] W. Jost, Diffusion in solids, liquids, gases, Academic Press, New York, 1969 fifth printing.
[31] B.H.W.S. Jong, C.M. Schramm, V.E. Parziale, J. Am. Chem. Soc. 106 (1984) 4396–4402.
[32] S.P. Szu, M. Greenblatt, L.C. Klein, J. Non-cryst. Sol. 124 (1990) 91–100.
[33] A.R. West, Solid State Chemistry and its Applications, Wiley, New York, 1990.